JOURNAL OF MATERIALS SCIENCE 27 (1992) 4287–4293

Carbothermal synthesis of titanium nitride

Part I *Influence of starting materials*

G. V. WHITE, K. J. D. MACKENZIE
Chemistry Division, DSIR, Private Bag, Petone, New Zealand
J. H. JOHNSTON
Chemistry Department, Victoria University of Wellington, New Zealand

Studies of the reactivity of six TiO_2 samples (two rutiles and four anatases) and nine carbon samples towards the formation of TiN by reduction of TiO_2 with carbon in a nitrogen atmosphere at 1150 °C show that the reaction is influenced by the chemical and physical properties of both the TiO_2 and the carbon. Although anatases and rutiles behave similarly, their reactivities are adversely affected by the presence of impurities such as those deliberately added as surface coatings in pigment-grade TiO_2. There is some evidence that the reactivity of the TiO_2 increases with increasing surface area. Carbons with higher ash contents appear to be more reactive. The reactivity of the carbons generally increases with increasing surface area, as measured by gas penetration methods (BET nitrogen adsorption and Blaine gas permeation).

1. Introduction

Titanium nitride is classed as an advanced ceramic material, the hardness and abrasion resistance of which makes it eminently suitable for engineering applications, especially as thin hard coatings on metal machining tools. Other applications include its incorporation as a dispersed powder in "hard metal"-containing ceramic–metal composites, and as a decorative coating on jewellery. Its metallic-type electrical conductivity makes it a useful component of electrically conducting ceramics for self-heating crucibles and ceramics which can be shaped by electro-discharge machining, but the high melting point of TiN (~ 2950 °C) makes fabrication of pure monolithic articles by hot pressing difficult, and the products tend to be porous [1]. Titanium nitride has also been proposed as an oxygen-free starting material for the production of titanium metal by electrolytic reduction in a molten salt bath [2], or for the synthesis of titanium boride by solid-state reaction with boron, which should be more controllable and less violent than the more usual reaction with titanium metal [3].

Several preparative methods can be used for titanium nitride.

(i) The reaction of titanium metal powder with nitrogen gas is capable of producing a pure powder product [4]. Variations of the method include physical vapour deposition (PVD), in which titanium metal (or some other titanium compound) is vaporized in a nitrogen plasma, or by low-pressure sputtering or electron beam evaporation under nitrogen, and deposited as a thin film of TiN on a substrate heated to 200–500 °C. These PVD methods for producing thin films have been discussed by Vaidyanathan [5] and Dearnley and Bell [6]. Another variation, in which the product is a mixture of nitrogen-deficient titanium nitride (TiN_{1-x}) and titanium metal phases, involves ignition of titanium metal powder in a self-propagating high-temperature synthesis (SHS) process which is sustained by the exothermic nature of the nitridation [7].

(ii) In the reaction of titanium metal powder with sodium azide, the solid reactants are ignited in a nitrogen atmosphere, the sodium being volatilized during the combustion [4].

(iii) The reaction of titanium hydride with ammonia which produces a high-purity product [8].

(iv) The reaction of titanium tetrachloride with a mixture of hydrogen and nitrogen [9] or ammonia and hydrogen [10] is used to deposit thin coatings by chemical vapour deposition (CVD) on substrates heated to $\geqslant 1000$ °C.

(v) In the reaction of sodium titanate with sodium azide, some of the product is in the form of whiskers [11].

(vi) Carbothermal reduction of titanium oxide involves the reduction of the oxide by heating with carbon powder in a nitrogen atmosphere, which simultaneously nitrides the reaction product. The overall reaction can be written

$$TiO_2 + 2C + \tfrac{1}{2}N_2 \rightarrow TiN + 2CO \qquad (1)$$

Although this method does not produce a product of high purity, one advantage of carbothermal reduction is the inexpensive nature of the raw materials (especially if pigment-grade TiO_2 is available, as it is in New Zealand, where it is recovered from locally occurring ilmenite). Another advantage of this preparative method is its potential for producing a range of intermediate solid solutions with titanium carbide, which also have applications as engineering ceramics. However, to control the reaction products so precisely

0022–2461

TABLE I Raw materials used in this investigation

Sample	Description and source	Total non-TiO_2 oxides (%)	Median particle size (μm)	Blaine surface area ($cm^2 g^{-1}$)	Calculated surface area[a] ($m^2 g^{-1}$)	BET Surface area ($mg g^{-1}$)	Reactivity index
R1	Rutile, Victoria University, Batch BH14/R1	0.9	1.0			2.2	92
R2	Rutile, Pigment grade, coated with SiO_2 and Al_2O_3, Dupont	3.7	0.56			12.0	16
A1	Anatase, paper coating grade, SCM	0	0.33			10.0	100
A2	Anatase, $\leqslant 0.01\%$ contaminants, J. T. Baker, Lot 31310	0.5	0.9			7.7	75
A3	Anatase, Victoria University, Batch BH12/125/Bulk	2.4	0.48			6.9	47
A4	Anatase, as A3, micronized, Batch BH21/51, 52, 53	1.5	0.52			3.1	73
C1	Lampblack, Baird and Tatlock			7500	0.56	6.2	77
C2	Graphite			4900	[b]	—	6
C3	Bituminous Coal, Stockton Mine, New Zealand			2000	[b]	0.7	30
C4	Carbon pigment, TintaCarb 300, Australian Carbon Black Pty Ltd			7300	0.69	72	39
C5	Carbon Pigment, FEF, Australian Carbon Black Pty Ltd			4700	1.0	42	22
C6	Anode Carbon, ex-coal, calcined 375 °C, Buller Mine, New Zealand			900	[b]	1.7	3
C7	Activated Carbon, ex-coconut shells, Taylors Christchurch (NZ) Ltd			3700	0.54	1190	65
C8	Activated Charcoal, acid washed, for decolouring, BDH			7900	0.40	880	68
C9	Decolouring Charcoal, J. T. Baker Chemicals Ltd			10200	0.34	1100	100

[a] Calculated from particle size distribution.
[b] Not available at time of publication.

TABLE II Chemical analyses of reactant titanium oxides

Sample	Component (%)					Total non-TiO_2 oxides in reaction mixture
	TiO_2	SiO_2	Al_2O_2	MgO	K_2O	
R1	99.1	0.6	–	–	0.3	0.31
R2	96.3	6.0	3.7	–	–	3.7
A1	100	–	–	–	–	0
A2	99.5	0.5	–	–	–	0.19
A3	97.6	1.2	0.4	0.4	0.2	0.92
A4	98.5	1.0	–	–	0.5	0.61

requires considerably better knowledge of the influence of the variable reaction parameters than is presently available, despite investigations going back to 1824 [12].

The aim of this work was, therefore, to clarify a number of aspects of the reaction of Equation 1, including the effect of the starting materials, the nature and stability of the intermediate phases and the kinetics, thermodynamics and mechanism of the overall reaction. In Part I of this work, the relative reactivities of a number of different starting materials are investigated, and the effects of parameters such as impurities, particle size and the polymorphic form of the TiO_2 are reported.

2. Experimental procedure

2.1. Materials

Nine different carbon samples ranging from activated carbon to powdered bituminous coal, and six TiO_2 samples (two rutiles and four anatases) were investigated. The details of these samples are shown in Table I, which includes the ash contents of the carbons, determined by weight loss after heating at 1000 °C in air for 1 h. Tables II and III present the chemical analyses of the TiO_2 samples and of the carbon ashes, respectively, determined by energy dispersive analysis of X-rays (EDX) using a Cambridge Stereoscan 250 Mk II scanning electron microscope with a Link 860 Series 2 energy-dispersive X-ray analyser system. The size and shape of the raw material particles was assessed by SEM (Cambridge Stereoscan 250 Mk II) and TEM (Philips EM420ST).

Surface-area measurements were made by the BET nitrogen adsorption method, using a Quantasorb Quantachrome apparatus. Relative surface areas were also measured by a modified Blaine permeametry method [13] which determines the flow rate of air through a powder compact. This measurement was made because its methodology seems to be relevant to the gas–solid carbothermal reduction reaction. Particle size distributions of the TiO_2 and carbon samples (Table I) were determined on samples ultrasonically dispersed in distilled water using a Malvern Mastersize MS20 laser diffraction apparatus.

2.2. Heating experiments

Intimate mixtures of the various carbons and titanium oxides were prepared containing carbon in excess of

TABLE III (a) Chemical analyses of carbon ashes (by EDX) and (b) oxide content contributed to reaction mixture by the carbons

(a)

Sample	Component (%)											
	TiO_2	SiO_2	Al_2O_3	MgO	SO_2	K_2O	Na_2O	CaO	MnO	Fe_2O_3	CuO	Ash content[a]
C1	–	7	1	7	3	–	–	73	2	5	–	4.9
C2	3	11	3	–	2	–	–	40	4	37	2	0.54
C3	1	53	18	3	2	2	1	6	–	10	–	1.8
C4	2	18	3	15	–	–	–	36	–	24	–	0.08
C5	3	27	–	9	–	–	–	28	–	32	–	0.46
C6	4	10	66	–	–	1	–	5	–	14	–	0.55
C7	–	13	42	–	9	18	4	1	4	10	–	3.39
C8	2	32	11	–	–	6	1	23	4	17	–	0.65
C9	–	26	11	1	–	1	12	1	–	5	–	7.25

(b)

Sample	Component (p.p.m.)											
	TiO_2	SiO_2	Al_2O_3	MgO	SO_2	K_2O	Na_2O	CaO	MnO	Fe_2O_3	CuO	Total
C1	–	792	163	782	311	–	–	8207	171	551	–	11 276
C2	–	131	34	–	21	–	–	500	–	457	28	1 170
C3	46	2202	748	125	87	83	29	228	4	415	–	4 004
C4	3	33	6	28	–	1	–	66	–	43	–	185
C5	36	291	–	101	–	–	–	292	–	342	–	1 062
C6	45	133	835	–	–	11	–	66	–	180	–	1 269
C7	–	980	3271	–	739	1387	289	97	297	764	–	7 824
C8	25	484	159	–	–	86	13	349	55	252	–	1 500
C9	–	4381	1923	247	–	161	1929	242	–	827	–	16 730

[a] Ashed in air at 1000 °C for 16 h.

the theoretical mole ratio TiO_2/C of 1:2. The additional carbon is necessary to counteract the effect of moisture and contaminating oxygen in the instrument-grade nitrogen gas, which typically contains 7 p.p.m. O_2, 3 p.p.m. CO_2 and 10 p.p.m. H_2O. Experiments with hand-mixed samples brushed through a 150 μm screen were found to produce similar results to mixtures milled with ethanol in a planetary ball mill with tungsten carbide balls; the hand grinding method was therefore adopted.

The relative reactivities of the various reactants were estimated as follows. Mixtures of all the titanium oxides with carbon C8 were reacted for 4 h at 1150 °C in ceramic boats placed in an electric tube furnace under a flowing nitrogen atmosphere ($0.1\ l\,min^{-1}$). The reactivities of the carbons were measured in mixtures with anatase A1 fired as above. After heating, the degree of TiN formation in all the mixtures was estimated by quantitative X-ray powder diffraction (see below). The six most reactive carbon samples all produced 100% TiN after 4 h heating; a further set of 1 h firings was thus necessary to distinguish the relative reactivities of these carbons. The reactivity indices for each reactant are the amounts of TiN formed, estimated from X-ray diffraction (XRD) peak heights, expressed as a percentage of the highest value.

2.3. Quantitative X-ray analysis (QXRD)

Normally, an internal standard for QXRD analysis is added in known weight proportion after firing and before analysis. This was not possible in the present experiment because the final carbon content varied with each firing, due to reaction with the variable oxygen contaminants present in the apparatus. Thus, the unusual step was taken of adding an inert internal standard before firing. A suitable standard was found by experiment to be α-Al_2O_3 (corundum), because, at the reaction times and temperatures used in this work, it neither reacts with the sample mixtures, nitrides or changes its X-ray character. Furthermore, the diffraction lines of corundum do not seriously interfere with those of TiN, nor of any other intermediate phases encountered in the reaction sequence. Although very fine corundum powder (< 0.3 μm) was too reactive to be used, BDH analytical grade Al_2O_3 was found to be suitable. The X-ray measurements were made using a Philips PW1700 computer-controlled diffractometer. The calibration standards were prepared using commercial TiN diluted with Ti_3O_5, the latter phase having been found most commonly to coexist with TiN in the partially reacted systems (see Part II [14]). The Ti_3O_5 phase for calibration was synthesized by heating rutile for 17 h at 1250 °C under hydrogen gas. The analyses were made using the heights of the TiN peak at $d = 0.212$ nm and the Al_2O_3 peak at $d = 0.209$ nm. The calibration curve is linear, passing through the origin. To correct for broadening of the TiN peaks in reaction mixtures at low concentration, the integral breadth of the TiN peak was also measured, and the product of the peak height and integral breadth used as a measure of the TiN content.

3. Results and discussion

3.1. Reactivity of the TiO_2 samples

Fig. 1 shows the negative correlation between reactivity and total non-TiO_2 oxide content of the samples. The precise oxide which is contributing to the decrease in reactivity is not apparent from inspection of the chemical analyses of the titanias, because there are insufficient data for most of the individual oxides. In the six samples investigated, there was measurable SiO_2, which correlates in a similar manner with the decrease in reactivity. There may, however, be no single chemical species which particularly interferes with the reactivity of the oxides, but the contaminants present may simply act as a physical barrier to the entry of nitrogen gas and exit of carbon monoxide from the individual particles.

The physical properties of the titanias such as the particle size and surface area were expected to show strong correlations with the reactivity, but this did not prove to be the case. There is a poor correlation with the median particle size (Fig. 2). On this diagram are also plotted several additional samples which were included in an initial broad survey, but which were not investigated in detail. These included several other commercial pigment-grade rutile samples, and a suite of the commercial samples which were chemically treated to remove the surface coatings which are applied to pigment-grade anatases and rutiles to aid miscibility. No obvious relationship exists with the BET surface area. No systematic differences in behaviour were noted between the rutile and anatase samples, all of which were shown by TEM to be of similar particle morphology, with fairly uniform shape and size; the rod or lath-like morphology of the rutile samples was not very pronounced, and no change in morphology or state of aggregation was noted in the washed samples.

3.2. Reactivity of the carbon samples

Fig. 3 shows the reactivity of the carbon samples as a function of the ash content indicating that in general the more reactive carbons have more ash. Further, the reactivity index is found to correlate to some extent with the SiO_2, Fe_2O_3 and K_2O contents of the ashes, the higher reactivities tending to occur with carbons which contribute more of these elements to the reaction mixture. Figs 4 and 5 show the relationship between reactivity and Fe_2O_3 and SiO_2 contents, respectively. Although the higher-ash carbons appear to be more reactive, their use in the present reaction is not desirable, in the interests of purity of the product, (although the presence of small amounts (2%) of impurities such as Al_2O_3 have been claimed to assist the high-temperature sintering of TiN [15]. Conversely, the presence of CaO has been claimed to inhibit TiN sintering [16]).

Relationships between the reactivity of the carbons and the surface areas measured by BET nitrogen adsorption and Blaine gas permeametry are shown in Figs 6 and 7, respectively. The better correlation with Blaine permeametry is unexpected; because the BET technique measures the surface accessible to gaseous nitrogen it might be expected to be the better predictor of reactivity. However, the Blaine measurement reflects the area accessible to the gas flowing through a

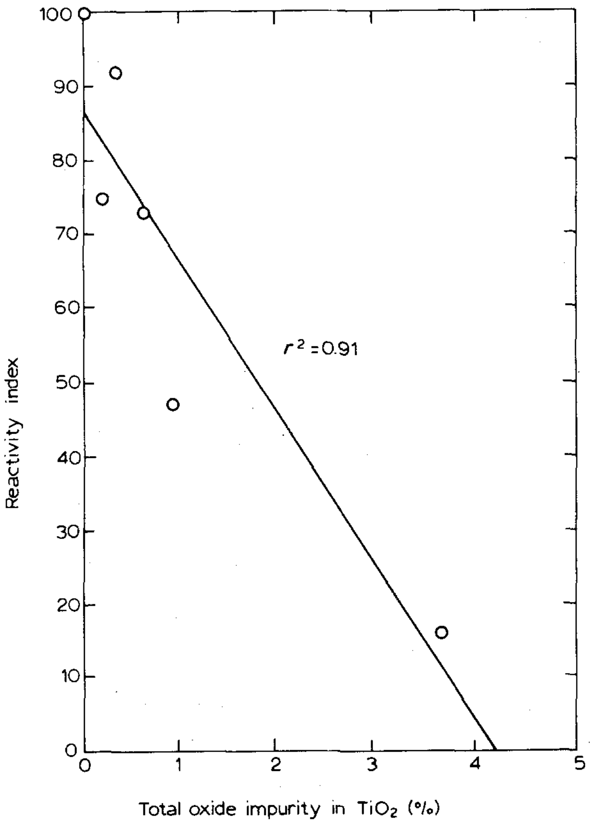

Figure 1 Relationship between the reactivity and the total impurity content of the titanium oxide starting materials, using carbon C8.

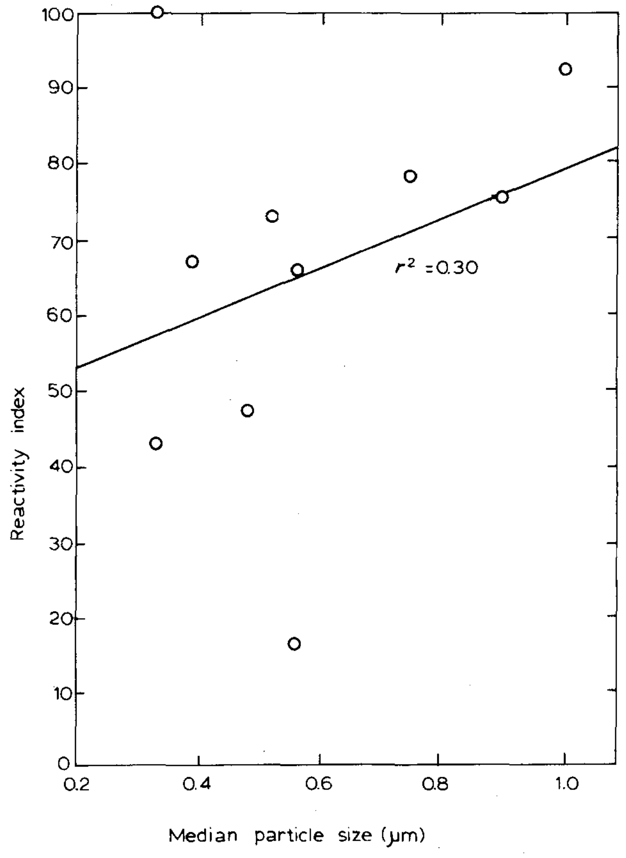

Figure 2 Relationship between the reactivity and the median particle size of the titanium oxide starting materials, using carbon C8.

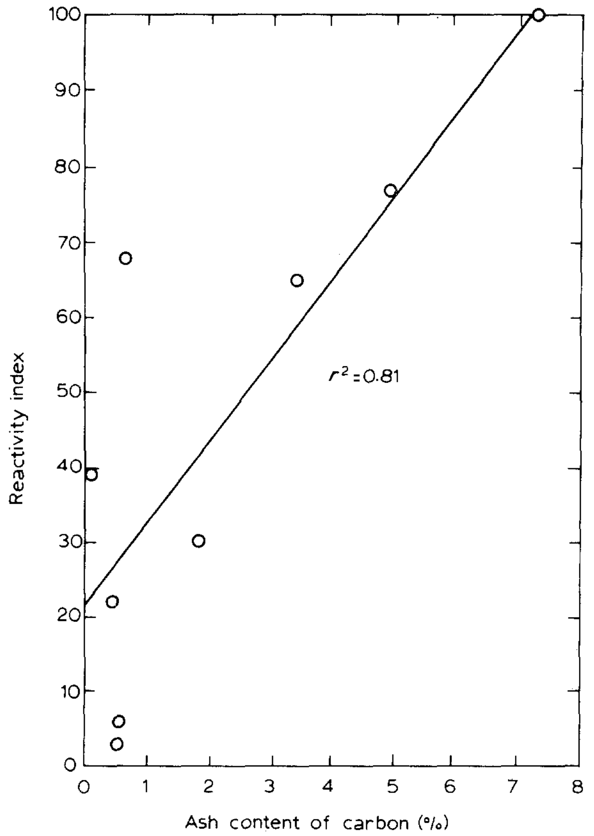

Figure 3 Relationship between the reactivity and the ash content of the carbon starting materials, using anatase A1.

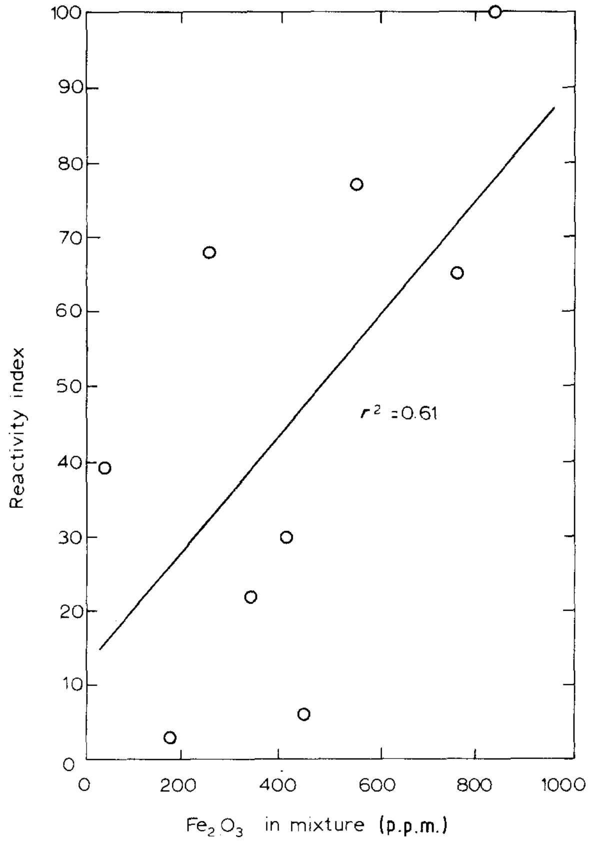

Figure 4 Relationship between the reactivity and the Fe_2O_3 content of the reaction mixture originating from the carbon starting materials, using anatase A1.

compact of particles and apparently better represents the situation in the sample mixture.

Fig. 8 shows the relationship between reactivity and the surface area of the carbon particles calculated from

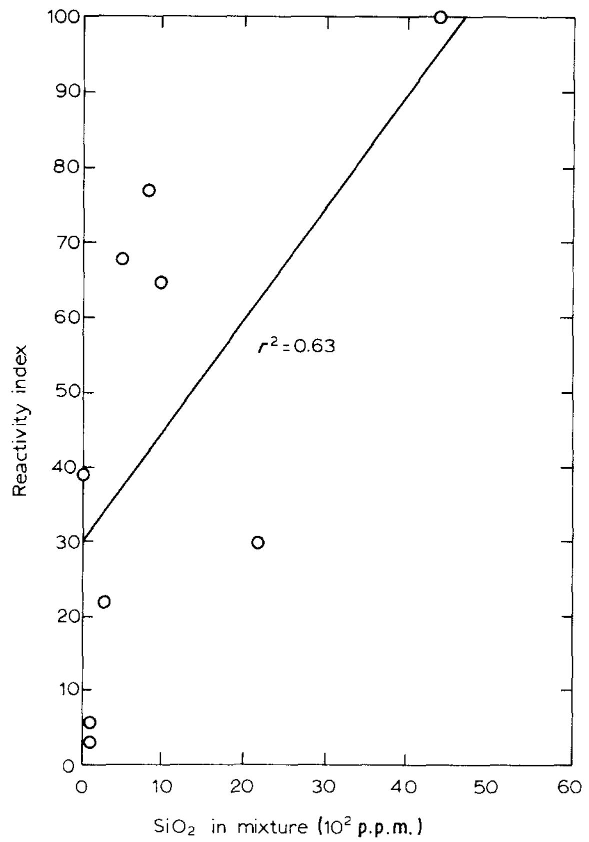

Figure 5 Relationship between the reactivity and the SiO_2 content of the reaction mixture originating from the carbon starting materials, using anatase A1.

the particle size distribution. The trend to lower reactivity with increasing surface area is unexpected; the method of calculation is, however, based on the assumption of spherical particles and is therefore the least realistic of the three surface-related parameters measured here. Although the detailed morphologies of the carbon particles were not examined, their scanning electron micrographs clearly reflect their various origins (two were prepared from charred wood, one was made from coconut shells, two were the sooty product of burnt oil or acetylene, two were coal by-products and one was a well-ordered crystalline graphite). On the basis of its high reactivity and low ash content, carbon C8 was chosen for the further experiments reported in Parts II and III [14, 17].

4. Conclusions

The reactivity of TiO_2 involved in carbothermal reduction is adversely affected by the presence of other oxides such as those deliberately added to pigment-grade TiO_2, principally as surface coatings to aid flow properties and dispersion. Insufficient data exist to indicate whether any particular contaminating oxide species decreases the reactivity. There are no obvious differences in the behaviour of the polymorphs anatase and rutile. The median particle size and the calculated surface area of the samples both show some correlation with activity, which increases with increasing surface area.

The reactivities of the carbon samples appear to be related to the ash content, carbons with higher ash

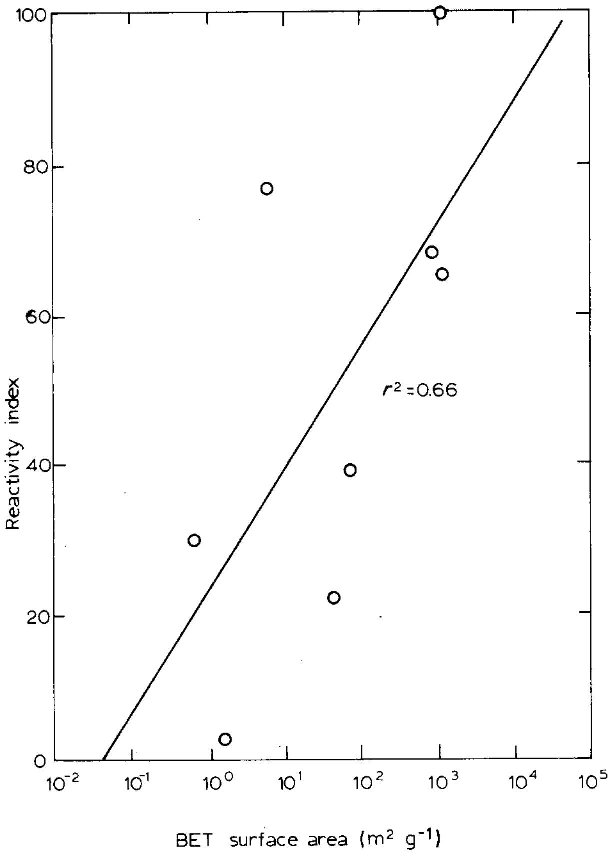

Figure 6 Relationship between the reactivity and the BET surface areas of the carbon starting materials, using anatase A1.

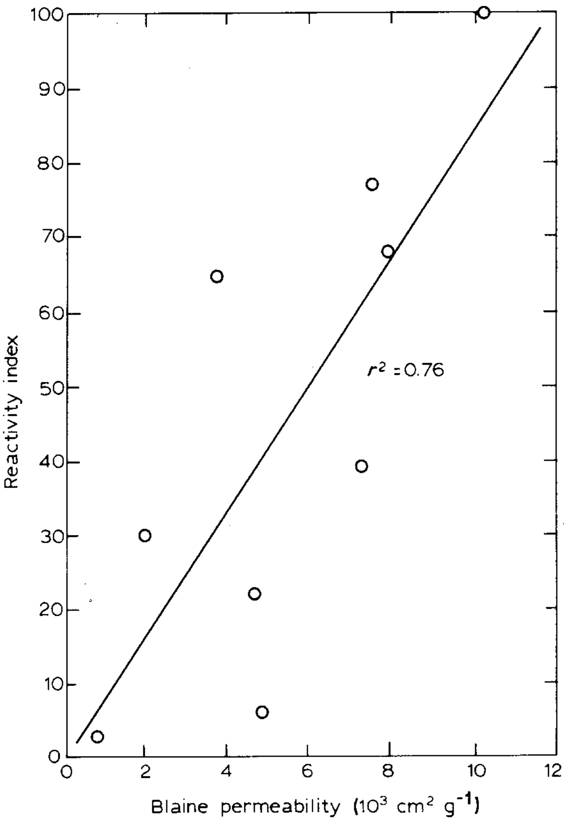

Figure 7 Relationship between the reactivity and the Blaine gas permeability of the carbon starting materials, using anatase A1.

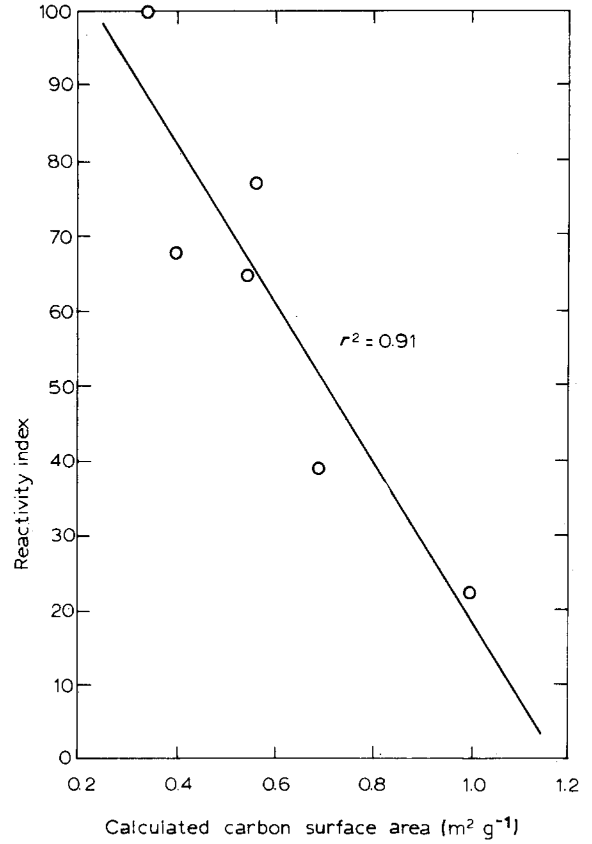

Figure 8 Relationship between the reactivity and the surface area of the carbon starting materials, calculated from particle size distribution data (anatase A1 was used).

contents being more reactive. The components of the ash which contribute to its particular reactivity could not be identified, but there is some indication that SiO_2 and Fe_2O_3 exert positive influences on the reactivity. The reactivity of the carbons generally increases with their surface area, as measured both by BET nitrogen adsorption and by the Blaine gas permeation method, but decreases with increasing surface area, as calculated from the particle size distribution. The latter calculation is based on the assumption of spherical particles, which is probably unwarranted in the present series of carbons originating from diverse sources.

Acknowledgements

We are indebted to Fletcher Titanium, New Zealand Coal Research Association, Mr D. Carter and Mr M. Schofield for supplying raw material samples, to Mrs K. Card for the SEM/EDX measurements, Dr N. Tapp for assistance with the BET measurements, and to Mr M. Ryan for the Blaine measurements.

References

1. J. B. HOLT, US Pat. 4622215 (1984).
2. E. K. KLEEPSIES and T. A. HENDRIE, US Bur. Mines Report 6447 (1964).
3. T. MATSUDAIRA, H. ITOH, S. NAKA, H. HAMAMOTO and M. OBAYASHI, *J. Mater. Sci.* **23** (1988) 288.
4. K. AGTE and K. MOERS, *Z. Anorg. Allgem. Chem.* **198** (1931) 233.
5. P. N. VAIDYANATHAN, *Ceram. Engng Sci. Proc.* **9** (1988) 1209.
6. P. A. DEARNLEY and T. BELL, *ibid.* **9** (1988) 1137.
7. A. Z. MUNIR, S. DEEVI and M. ESLAMOO-GRAMI, *High Temp. High Press.* **20** (1988) 19.

8. P. DUWEZ and F. ODELL, *J. Electrochem. Soc.* **97** (1950) 299.
9. A. DOI, N. FUJIMORI and T. YOSHIOKA, *Inst. Phys. Conf. Ser.* **75** (1986) 743.
10. Z. LIANXI, J. PONG and R. JUNGUO, *Chengdu Keji Daxue Xuebao* (1985) 65.
11. C. E. BAMBERGER, *Powder Diff.* **3** (1988) 240.
12. H. ROSE, quoted in J. W. MELLOR, "A Comprehensive Treatise on Inorganic and Theoretical Chemistry", Vol. VII (Longmans, London, 1972) p. 43.
13. N. F. SHULZ, *Int. J. Min. Proc.* **1** (1974) 65.
14. G. V. WHITE, K. J. D. MACKENZIE, I. W. M. BROWN, M. E. BOWDEN and J. H. JOHNSTON, *J. Mater. Sci.* **27** (1992) 4294.
15. M. B. BEVER (ed.), "Encyclopaedia of Materials Science Engineering" (Pergamon, London, 1986) p. 3206.
16. P. P. ALEXANDER, US Pat. 2461018 (1949).
17. G. V. WHITE, K. J. D. MACKENZIE, I. W. M. BROWN and J. H. JOHNSTON, *J. Mater. Sci.* **27** (1992) 4300.

Received 23 April
and accepted 5 August 1991